$$+\frac{11}{600r^3}-\frac{3}{640r^4}-\frac{13}{2400r^5}+\frac{1}{480r^6}+A_3^2\left(r^3+\frac{3}{4r^4}\right)\Bigg]$$
$$+\sum_{n=4}^{\infty}A_n^2\left(r^n+\frac{n}{n+1}\frac{1}{r^{n+1}}\right)P_n(\mu) \quad \text{(A-27)}$$

The inner result may now be written in a form good to $O(\epsilon^2)$. As usual, this may be rewritten in (ρ, μ), expanded for small ϵ, and terms up to and including $O(\epsilon^2)$ may be retained for the match.

We have:

$$\text{4-outer (3-inner) } t=\left(r+\frac{1}{2r^2}\right)P_1(\mu)+\epsilon\left[\frac{1}{12r}-\frac{1}{6r}P_2(\mu)\right]$$
$$+\epsilon^2\Bigg[A_0^2+\left(A_1^2r-\frac{79}{1200}\right)P_1(\mu)+A_2^2r^2P_2(\mu)$$
$$+\left(A_3^2r^3+\frac{23}{2400}\right)P_3(\mu)+\sum_{n=4}^{\infty}A_n^2r^nP_n(\mu)\Bigg] \quad \text{(A-28)}$$

Similarly, the $O(\epsilon^2)$ outer solution, rewritten in inner variables, expanded for small ϵ, and truncated to include terms up to $O(\epsilon^2)$ is given below.

$$\text{3-inner (4-outer) } T^*=\left(r+\frac{1}{2r^2}\right)P_1(\mu)+\epsilon\left[\frac{1}{12r}-\frac{1}{6r}P_2(\mu)\right]$$
$$+\epsilon^2\left[-\frac{9}{160}-\frac{79}{1200}P_1(\mu)+\frac{23}{2400}P_3(\mu)\right] \quad \text{(A-29)}$$

It is clear that the terms up to $O(\epsilon)$ already have been matched, and the coefficients of ϵ^2 may now be matched to yield:

$$A_n^2=-\frac{9}{160}\delta_{n0} \quad \text{(A-30)}$$

Introduction of Eq. A-30 in Eq. A-27 leads to a final result for $t_2(r, \mu)$ which is reported in Eq. 50 of the text.

LITERATURE CITED

Abramowitz, M., and I. Stegun, *Handbook of Mathematical Functions*, Dover, New York, NY (1968).

Acrivos, A., and T. D. Taylor, "Heat and Mass Transfer from Single Spheres in Stokes Flow," *Phys. Fluids*, **5**, No. 4, 387 (1962).

Bratukhin, Y. K., "Thermocapillary Drift of a Viscous Fluid Droplet," *Izveztiya Akademii Nauk* SSSR, Mekhanika Zhiokosti, Gaza, No. 5, 156 (1975); original in Russian, NASA Technical Translation NASA TT 17093 (June, 1976).

Goertzel, G., and N. Tralli, *Some Mathematical Methods of Physics*, McGraw-Hill, New York (1960).

Happel, J., and H. Brenner, *Low Reynolds Number Hydrodynamics*, Prentice-Hall, Englewood Cliffs, NJ, 133 (1965).

Hardy, S. C., "The Motion of Bubbles in a Vertical Temperature Gradient," *J. Colloid Interface Sci.*, **69**, No. 1, 157 (1979).

Kaplun, S., "The Role of Coordinate Systems in Boundary-Layer Theory," Z. Agnew, *Math. Phys.*, **5**, 111 (1954).

Kaplun, S., and P. A. Lagerstrom, "Asymptotic Expansions of Navier-Stokes Solutions for Small Reynolds Numbers," *J. Math. Mech.*, **6**, 585 (1957).

Levan, M. D., and J. Newman, "The Effect of Surfactant on the Terminal and Interfacial Velocities of a Bubble or Drop," *AIChE J.*, **22**, No. 4, 695 (1976).

Levich, V. G., and A. M. Kuznetsov, "Droplet Motions in Liquids Caused by Surface Active Substances," *Doklady Akademii Nauk SSSR*, **146**, No. 1, 145 (1962).

Levich, V. G., *Physicochemical Hydrodynamics*, Prentice-Hall, Englewood Cliffs, NJ (1962).

McGrew, J. L., T. L. Rehm, and R. G. Griskey, "The Effect of Temperature-Induced Surface Tension Gradients on Bubble Mechanics," *Appl. Sci. Res.*, **29**, 195 (1974).

Naumann, R. J., ed., *Descriptions of Experiments Selected for the Space Transportation System (STS) Materials Processing in Space Program*, NASA TM-78175 (1978).

Nielson, G. F., and M. C. Weinberg, "Outer Space Formation of a Laser Host Glass," *J. Non-Crystalline Solids*, **23**, No. 1, 43 (1977).

Proudman, I., and J. R. A. Pearson, "Expansions at Small Reynolds Numbers for the Flow Past a Sphere and a Circular Cylinder," *J. Fluid Mech.*, **2**, 237 (1957).

Smith, H. D., D. M. Mattox, W. R. Wilcox, and R. S. Subramanian, "Glass Fining Experiments in Zero Gravity," Westinghouse R&D Document No. 77-906-FINES-R5 to Marshall Space Flight Center (June, 1977).

Van Dyke, M., *Perturbation Methods in Fluid Mechanics*, The Parabolic Press, Stanford, CA (1975).

Wilcox, W. R. et. al., "Screening of Liquids for Thermocapillary Bubble Movement," *AIAA J.*, **17**, No. 9, 1022 (1979).

Young, N. O., J. S. Goldstein, and M. J. Block, "The Motion of Bubbles in a Vertical Temperature Gradient," *J. Fluid Mech.*, **6**, 350 (1959).

Manuscript received May 2, 1980; revision received September 18, and accepted October 20, 1980.

Kinetics of Nonisothermal Sorption: Systems with Bed Diffusion Control

A theoretical model is presented to describe the kinetics of nonisothermal sorption for a system in which the main resistance to mass transfer is the macrodiffusional resistance of the absorbent particle bed while the main resistance to heat transfer is the resistance at the external surface of the adsorbent sample. The model is used to interpret experimental kinetic data for the sorption of several hydrocarbons in 10X and 13X zeolite crystals. By varying the configuration of the sample bed and the size of the zeolite crystals it is shown that, for n-heptane and iso-octane in 13X, the intracrystalline diffusional resistance is negligible even in 40-μm crystals. The assumption of intracrystalline diffusion control which has been made in earlier kinetic studies of similar systems is therefore incorrect.

D. M. RUTHVEN

and

LAP-KEUNG LEE

Department of Chemical Engineering
University of New Brunswick
Fredericton, N.B., Canada

SCOPE

Sorption kinetics in zeolite crystals have generally been considered to be controlled by diffusion within the micropores of the zeolite framework, although the influence of heat transfer resistance has been recognized. For sorbates such as hydrocarbons in small port zeolites such as type A, this assumption is probably correct at least in relatively large zeolite crystals. In the more open lattice of the faujasite zeolites intracrystalline diffusion is much faster, so that other rate processes such as the

diffusion of the sorbate into the adsorbent sample bed become relatively more important. We report here a theoretical analysis of the problem of nonisothermal sorption for a system in which the major resistance to mass transfer is the diffusional resistance of the sample bed while the major heat transfer resistance is at the external surface of the sample. A detailed analysis of experimental uptake rates for heptane and isooctane in a series of different sized 13X zeolite crystals (3-40 μm) with different sample bed configurations confirms the validity of the theoretical model.

CONCLUSIONS AND SIGNIFICANCE

Uptake rates for medium molecular weight saturated hydrocarbons in type-X zeolite crystals are controlled by the combined effects of heat transfer and diffusion into the adsorbent bed rather than by intracrystalline (zeolitic) diffusion. Even with very small adsorbent samples spread thinly (~5-10) monolayers) over the sample pan and with relatively large zeolite crystals (~40 μm), the diffusional resistance of the sample bed is greater than the intracrystalline resistance. The latter cannot, therefore, be measured in an uptake experiment and previous results, based on the assumption of intracrystalline control, are therefore invalid.

The nonisothermal model provides a good representation of the kinetic behavior of the systems studied and the parameters derived from the model (heat capacity, heat transfer coefficients and intercrystalline diffusivities) are consistent with *a priori* estimates. Except at very low pressures, the dominant mechanism of transport within the adsorption sample bed is molecular diffusion but at very low pressures the transition to the Knudsen region is observed.

Using the theoretical model and the approximate values of the parameters found in the present study it is possible to make a preliminary estimate of the bed diffusion and heat transfer resistances for any system for which the adsorbent sample configuration is known and equilibrium adsorption isotherms are available. Comparison with the experimental uptake curve will then show directly whether or not intracrystalline diffusional resistance is significant for the particular system and conditions. For small, commercial type-X zeolite crystals, the intracrystalline diffusional resistance for medium molecular weight hydrocarbons is insignificant under all practically important conditions.

In a previous paper (Ruthven, Lee and Yucel, 1980), we considered the influence of finite heat transfer resistance on the sorption kinetics for a system in which the main resistance to mass transfer is diffusion of the sorbate into the individual adsorbent particles. A somewhat different situation can also arise in which the major resistance to mass transfer is the macrodiffusion of sorbate into the adsorbent particle bed, rather than microdiffusion within the individual particles. This tends to occur when the particles are small (D_c/r^2 large) and the bed is deep (D_e/l^2 small). We here present a simple theoretical model to describe nonisothermal sorption kinetics under conditions of bed diffusion control. The model is used to interpret experimental uptake curves for sorption of several hydrocarbons in 10X and 13X zeolite crystals.

MATHEMATICAL MODEL

The adsorbent sample is represented as a parallel-sided, macroporous slab composed of the individual adsorbent particles with interparticle voids, into which sorbate can diffuse only through the free upper surface. We assume that intracrystalline diffusion is rapid so that the sorbate concentration throughout each individual adsorbent particle is always uniform. Both the thermal conductivity of the individual adsorbent particles and the effective thermal conductivity of the particle bed are assumed to be large enough to maintain an essentially uniform temperature throughout the entire adsorbent sample. The rate of heat transfer between adsorbent sample and ambient fluid, which is assumed to obey Newton's Law, is finite, so that during the course of the transient adsorption there is a time-dependent temperature difference between the adsorbent and ambient fluid. The system is subjected, at time zero, to a small differential step change in ambient sorbate concentration (pressure) from a previously established equilibrium condition. We assume that concentration equilibrium between fluid phase and adsorbed phase is established rapidly at the free surface of the sample and the equilibrium adsorbed phase concentration is assumed to vary linearly with both temperature and fluid phase concentration. This will always be a valid approximation for a sufficiently small concentration step.

Subject to these approximations, the system may be described by the following set of equations:

$$\frac{\partial q}{\partial \tau} = \frac{\partial^2 q}{\partial y^2} \tag{1}$$

$$q(y, o) = q_o, \quad q(1, \tau) = q_s, \quad \left.\frac{\partial q}{\partial y}\right|_{y=o} = o \tag{2}$$

$$\bar{q} = \int_o^1 q dy \tag{3}$$

$$\rho(-\Delta H)\frac{d\bar{q}}{d\tau} = \rho C p \frac{dT}{d\tau} + \frac{ha(T - T_o)}{(D_e/l^2)} \tag{4}$$

where the adsorbed phase concentration $q(y, \tau)$ is assumed to be uniform throughout an individual crystal and the effective diffusivity is defined by:

$$D_e = \frac{\epsilon D}{(1 - \epsilon)} \Big/ \left.\frac{\partial q^*}{\partial c}\right|_{T=T_o} \tag{5}$$

This model is seen to be formally the same as the model developed by Armstrong, Wellons and Stannett (1969) to describe nonisothermal sorption in a parallel sided polymer film.

The solution may be obtained by Laplace transformation:

$$\bar{Q} = \frac{\bar{q} - q_o}{q_\infty - q_o} = 1 - \sum_{n=o}^{\infty} \frac{2e^{-p_n^2 \tau}}{p_n^2 \cot p_n^2 (1 + 2/\beta) + p_n^2 + p_n \cot p_n} \tag{6}$$

$$\left(\frac{T - T_o}{q_\infty}\right)\frac{\partial q^*}{\partial T}$$

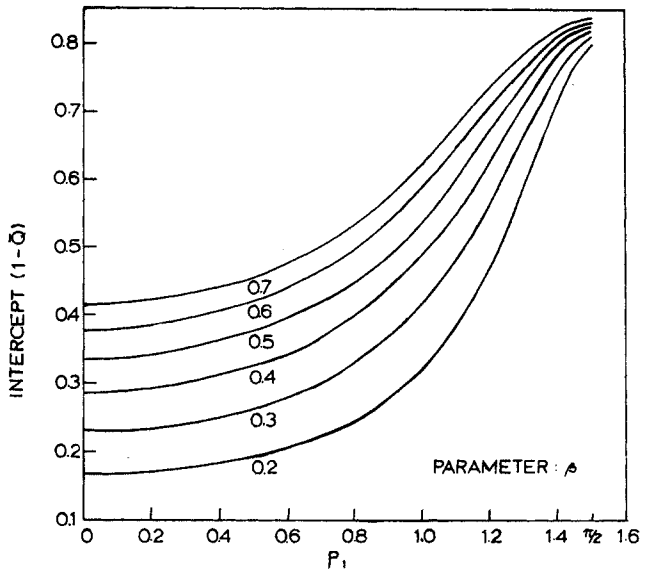

Figure 1. Intercepts $(1 - \bar{Q})$ of plots of $\ln(1 - \bar{Q})$ vs. t as function of p_1 calculated according to Eq. 6 for various values of β.

$$= \sum_{n=o}^{\infty} \frac{2e^{-p_n^2\tau}}{p_n \cot p_n(1 + 2/\beta) + 1 + p_n \tan p_n} \quad (7)$$

where the values of p_n are given by the roots of:

$$\cot p_n = \beta p_n/(\alpha - p_n^2) \quad (8)$$

These expressions give the uptake curve and the temperature history of the sample as a function of the dimensionless time variable $\tau(\equiv D_e t/l^2)$ with the parameters

$$\alpha \equiv \frac{ha/\rho C_p}{D_e/l^2} \text{ and } \beta = \frac{\Delta H}{C_p} \cdot \frac{\partial q^*}{\partial T}.$$

We have neglected the temperature dependence of D_e even though, because of the presence of the factor $\partial q^*/\partial c$, this can be quite strong. It has, however, been shown previously (Lee and Ruthven, 1979) that, provided consideration is restricted to a sufficiently small concentration step, the effect of the temperature dependence of the diffusivity will always be minor compared with the effect of the temperature dependence of the equilibrium adsorbed phase concentration.

In the long time region, only the first term ($p = p_1$) of the summation defined in Eq. 6 is significant so that, for all values of α and β a plot of $\ln(1 - \bar{Q})$ vs. τ will yield a straight line with slope $-p_1^2 D_e/l^2$ and intercept given by the pre-exponential factor in Eq. 6. Figure 1 shows the intercepts plotted against p_1 for various values of β. This plot provides the basis of a simple method for the analysis of experimental uptake curves, described below.

For isothermal sorption ($\beta = o$ or $\alpha \to \infty$) Eq. 8 reduces to $\cot p_n = 0$ which has a series of roots $p_n = (2n + 1)\pi/2$ or $p_n^2 = (2n + 1)^2\pi^2/4$, $n = 0, 1, 2 \ldots$. Eq. 6 then reduces to the familiar form for isothermal diffusion into a slab (Crank, 1958):

$$\bar{Q} = 1 - \frac{8}{\pi^2} \sum_{n=o}^{\infty} \frac{1}{(2n + 1)^2} \exp\{-(2n + 1)^2\pi^2\tau/4\} \quad (9)$$

When diffusion is rapid, the uptake rate is controlled entirely by heat transfer. The limiting behavior may be deduced by considering the asymptotic forms of Eqs. 6 and 8 for small values of α. Retaining only the first term of the series expansion $p_1 \tan p_1 = p^2 + p^4/3 + 2p^6/15 + \ldots$ shows that, for small α, the first root of Eq. 8 is given by $p_1^2 \approx \alpha/(1 + \beta)$ so that the asymptotic expression for the uptake curve is:

TABLE 1. DETAILS OF ZEOLITE CRYSTALS

Zeolite	Crystal Diam. (μm)	Origin	Sample wt. (mg)
13X	3	Linde	14-22
	24, 39	Yucel*	12-14
	17	Shdanov**	20-28
	55	Shdanov**	12-14
10X	1.5	Linde	51-63

* Samples were prepared by H. Yucel in this laboratory using Charnell's method (Charnell, 1971).

** Samples of zeolites prepared by S. P. Shdanov in Leningrad and provided by J. Karger (K.M.U., Leipzig).

$$1 - \bar{Q} = \frac{\beta}{1 + \beta} \cdot \exp\{-\alpha\tau/(1 + \beta)\}$$

$$= \frac{\beta}{1 + \beta} \exp\left\{\frac{-hat}{\rho C_p(1 + \beta)}\right\} \quad (10)$$

In the adiabatic limit ($\alpha = o$) Eqs. 6 and 8 reduce to:

$$\bar{Q} = 1 - \sum_{n=1}^{\infty} \frac{2e^{-p_n^2\tau}}{\beta(1 + \beta) + p_n^2} \quad (11)$$

$$\beta \tan p_n = -p_n \quad (12)$$

COMPARISON OF THEORY AND EXPERIMENT

Diffusion of saturated medium chain and cyclic hydrocarbons in 10X and 13X zeolite crystals is rapid and it appears that uptake rates are generally controlled by macrodiffusion and heat transfer, rather than by intracrystalline diffusion, even in relatively large (~40μm) crystals. Experimental uptake curves for several representative systems are analyzed below. Uptake curves were measured gravimetrically in a Cahn vacuum microbalance system and the concentration steps over which the uptake curves were measured were kept small in order to validate the approximations of the theoretical model. Details of the zeolite samples are given in Table 1 and the equilibrium isotherms are shown in Figures 2 and 3.

SORPTION OF *n*-HEPTANE AND ISO-OCTANE IN 13X ZEOLITE CRYSTALS

Figure 4 shows selected uptake curves for *n*-heptane-13X, measured over similar pressure steps but with different crystal sizes and sample bed configurations. Details are given in Table 2. It is evident that, for similar sizes of pan and sample weight, the uptake rates for the various crystal size fractions are similar and for a given crystal size the uptake rates are faster when the depth of the adsorbent bed is small (wide pan, small sample weight). These results are consistent with macro/heat transfer control since, if intracrystalline diffusion were the rate limiting process, the uptake rate would be independent of sample weight and pan width and inversely proportional to the square of the crystal radius.

2-2-4 trimethyl pentane (iso-octane) is more strongly adsorbed than *n*-heptane but the kinetic behavior is similar. Uptake curves measured under comparable conditions (similar sample weight, the same temperature and similar pressure step) with 24 μm and 39 μm 13X crystals are compared in Figure 5. It is evident that there is no significant difference between the curves for the two crystal sizes, indicating the absence of any significant intracrystalline diffusional resistance at least at the lower pressures and temperatures. For the larger crystals at higher pressures and temperatures there was evidence of some intracrystalline diffusion resistance.

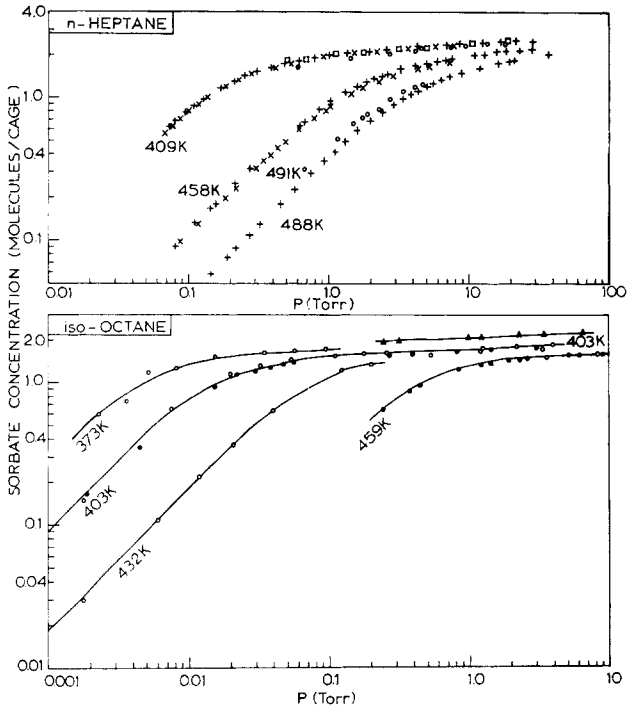

Figure 2. Equilibrium isotherms for sorption on n-heptane and iso-octane in 13X zeolite crystals. (○, 39μm Yucel; ●, 24μm Yucel; ▲, 55μm, Shdanov; ×, +, 17μm Shdanov—different sample configurations; □, 3μm Linde) (1 torr = 133.3 Pa).

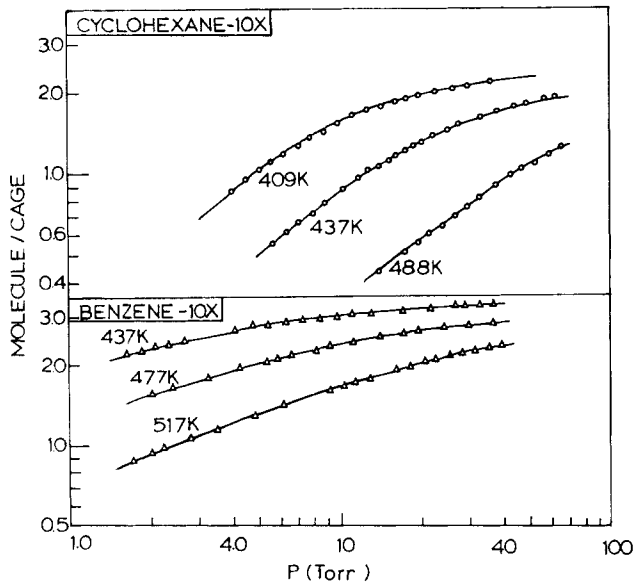

Figure 3. Equilibrium isotherms for sorption of cyclohexane and benzene in 10X zeolite crystals (1 torr = 133.3 Pa).

For small adsorbent bed depths and at the higher pressures and temperatures the macrodiffusional resistance is also small and the uptake curves conform closely to Eq. 10, the limiting expression for heat transfer control. This behavior is illustrated in Table 3 in which representative uptake curves are analyzed. Values of βC_p were calculated directly from the equilibrium data ($\beta C_p = \Delta H \cdot \partial q^*/\partial T$) and values of β and $ha/\rho C_p$ were derived from the slopes and intercepts of plots of $ln(1 - \bar{Q})$ vs. t, according to Eq. 10. The individual values of C_p, calculated by comparing the values of βC_p derived from the equilibrium data with the values of β from the uptake curves, show some scatter but there is no significant trend with sorbate concentration. The values obtained with the different sorbates are similar and consistent with the total heat capacity of the adsorbent sample, estimated as the sum of the heat capacity of the zeolite crystals

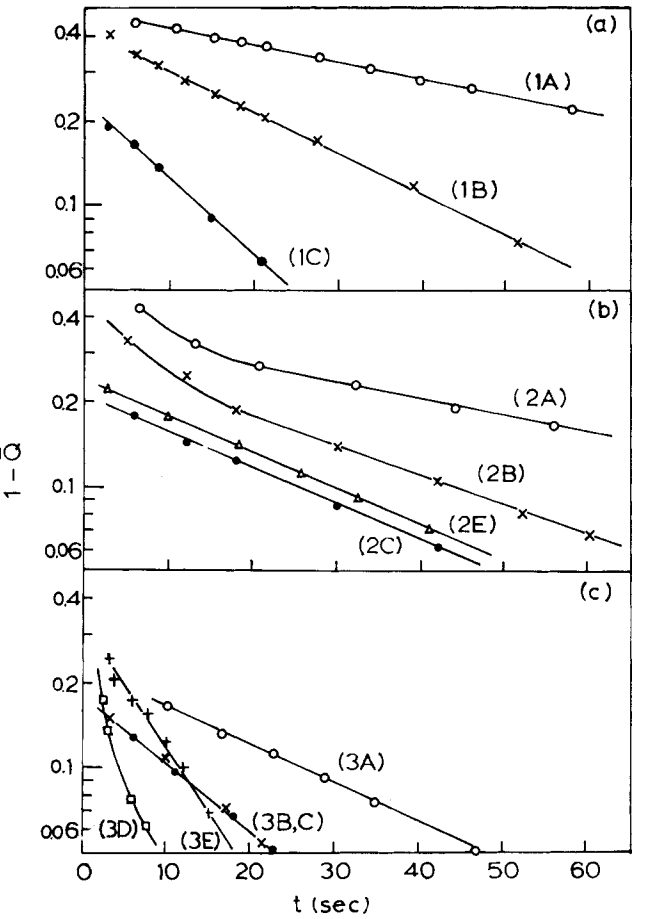

Figure 4. Comparison of uptake curves for sorption on n-heptane in 13X zeolite at 406-409°K. Uptake curves in each of the three figures (a, b, c) are measured over comparable pressure steps with different crystal sizes, sample weights and pan diameters as given in Table 2.
Series A: 17μm crystals, 20 mg sample, 0.5 cm pan
Series B: 17μm crystals, 28 mg sample, 1.0 cm pan
Series C: 3μm crystals, 20 mg sample, 1.5 cm pan
Series D: 3μm crystals, 14 mg sample, 2.0 cm pan
Series E: 39μm crystals, 14 mg sample, 0.7 cm pan

TABLE 2. COMPARATIVE UPTAKE CURVES FOR SORPTION OF n-HEPTANE IN 13X ZEOLITE AT 409°K WITH DIFFERENT CRYSTAL SIZES AND SAMPLE BED CONFIGURATIONS (FIGURE 4)

Curve No.	Pressure Step (Pa)	Conc. (molecule/cage)	$2r$ μm	Pan Diam. (cm)	Sample wt. (mg)	Time for 90% Uptake (s)
1a	13-16	0.97	17	0.5	20	113
1b	13-16	0.92	17	1.0	28	43
1c	13-21	—	3.0	1.5	22	13.5
2a	133-173	2.0	17	0.5	20	45
2b	120-200	2.0	17	1.0	28	22
2c	160-120	2.0	3.0	1.5	22	12.5
2e	80-187	1.61	39	0.7	14	15
3a	1000-1130	2.37	17	0.5	20	25
3b	760-1040	2.37	17	1.0	28	11
3c	1013-693	2.33	3.0	1.5	22	10.5
3d	1253-760	2.35	3.0	2.0	14	4.5
3e	600-986	2.23	39	0.7	14	11

Series 1, 2 and 3 denote comparable pressure steps. Runs (a) and (b) refer to the same 17-μm diameter crystals with two different sample weight and pan diameters. Runs (c) and (d) refer to the same Linde 13X crystals (3.0-μm diameter) with two different sample weights and pan diameters. Runs (e) refer to 39-μm diameter 13X crystals.

With small samples on the larger diameter pans, it is difficult to ensure a uniform depth of adsorbent sample so the pan width provides only an approximate indication of the effective bed depth.

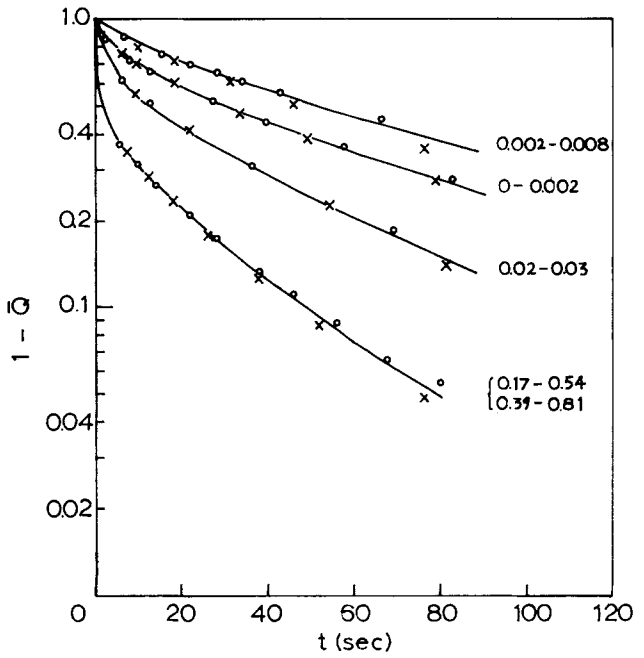

Figure 5. Comparison of uptake curves for iso-octane in 13X zeolite crystals at 403°K. (24μm crystals, ×; 39μm crystals, ○. Pressure steps in Torr are indicated on the curves. Sample wt. was 11-12 mg and pan diameter 0.7 cm) (1 torr = 133.3 Pa).

and the containing pan. Similarly, the values of $ha/\rho C_p$ are consistent and at the higher pressures are essentially independent of concentration. The numerical values of the heat transfer coefficients are consistent with the values estimated theoretically as the sum of the contribution from radiation and conduction in a stagnant gas. (See footnote to Table 6.)

At lower temperatures and pressures the bed-diffusional resistance becomes dominant and this effect is more pronounced for iso-octane than for heptane. This is to be expected since the macrodiffusional time constant (D_e/l^2) is inversely proportional to the isotherm slope (see Eq. 5) and the isotherm slope will be greatest at low temperatures and pressures and greater for iso-octane than for heptane. The presence of diffusional resistance could be easily detected when the uptake curves were analyzed in the above manner since when diffusional resistance is significant the apparent values of β derived from the intercepts of the plots of $\ln(1-\bar{Q})$ vs. t are erroneously large, leading to unreasonably low values of C_p. Furthermore, since the relative importance of diffusion and heat transfer resistances varies with sorbate concentration the apparent values of C_p which are obtained when diffusion resistance is significant are strongly concentration dependent. The uptake curves obtained under conditions such that both diffusion and heat transfer resistances are significant conform to Eq. 10. A representative set of such curves is shown in Figure 6 and the transition from near isothermal diffusion at low pressures to increasing heat transfer control at higher pressures is clearly evident from the shapes of the curves.

At low sorbate concentrations, within the Henry's Law region ($q^* = Kc$, $K = K_o \exp(-\Delta H/RT)$):

TABLE 3. ANALYSIS OF UPTAKE CURVES FOR SORPTION OF *n*-HEPTANE IN 'THIN' BEDS OF 13X ZEOLITE CRYSTALS UNDER CONDITIONS OF HEAT TRANSFER CONTROL (Eq. 10)

Pressure Step (Pa)	Concentration (molecule/cage)	Slope (s^{-1})	Intercept	βC_p ($J \cdot g^{-1} deg^{-1}$)	C_p ($J \cdot g^{-1} deg^{-1}$)	$ha/\rho C_p$ (s^{-1})
		n-Heptane, 28 mg of 17μm Diameter Crystals on 1.0-cm Pan at 458°K				
40-45	0.36	0.06	0.18	0.54	2.17	0.075
51-57	0.45	0.075	0.29	0.66	1.63	0.097
83-89	0.64	0.064	0.27	0.84	2.72	0.087
107-127	0.84	0.051	0.30	0.93	2.17	0.073
192-236	1.18	0.060	0.34	0.853	1.63	0.092
587-680	1.66	0.070	0.21	0.60	2.26	0.088
680-986	1.77	0.072	0.24	0.54	1.80	0.094
		n-Heptane, 13 mg of 39μm Diameter Crystals on 0.7-cm Pan at 491°K				
91-160	0.53	0.075	0.29	0.62	1.55	0.105
232-248	0.78	0.075	0.29	0.82	2.10	0.104
313-264	1.00	0.070	0.29	0.76	1.92	0.098
453-546	1.20	0.079	0.27	0.73	1.96	0.108
613-746	1.35	0.083	0.25	0.69	2.10	0.111
933-1133	1.51	0.111	0.21	0.59	2.21	0.141
1373-1600	1.62	0.129	0.22	0.51	2.26	0.15
2279-2640	1.76	0.125	0.22	0.44	1.5	0.16
		i-Octane, 12.4 mg of 24μm Crystals on 0.7-cm Pan at 459°K				
33-51	0.89	0.042	0.44	1.38	1.75	0.08
51-60	0.96	0.042	0.40	1.30	1.92	0.07
60-112	1.23	0.062	0.31	0.84	1.88	0.09
112-164	1.32	0.073	0.27	0.67	1.80	0.1
164-195	1.37	0.091	0.26	0.54	1.63	0.12
195-257	1.43	0.094	0.21	0.46	1.67	0.12
257-354	1.48	0.091	0.18	0.37	1.67	0.11
354-806	1.58	0.096	0.11	0.29	2.10	0.11
		i-Octane, 12.1 mg of 55μm Crystals on 0.7-cm Pan at 403°K				
52-161	2.11	0.086	0.145	0.31	1.86	0.10
161-316	2.16	0.096	0.105	0.23	1.96	0.11
316-466	2.20	0.103	0.096	0.22	2.10	0.11
466-866	2.24	0.112	0.083	0.19	2.05	0.12

These values of C_p are consistent with values estimated from $C_p = (C_p)_{\text{zeolite}} + \frac{\text{wt. of Zeolite}}{\text{wt. of Sample Pan}} \times (C_p)_{\text{Pan}}$.

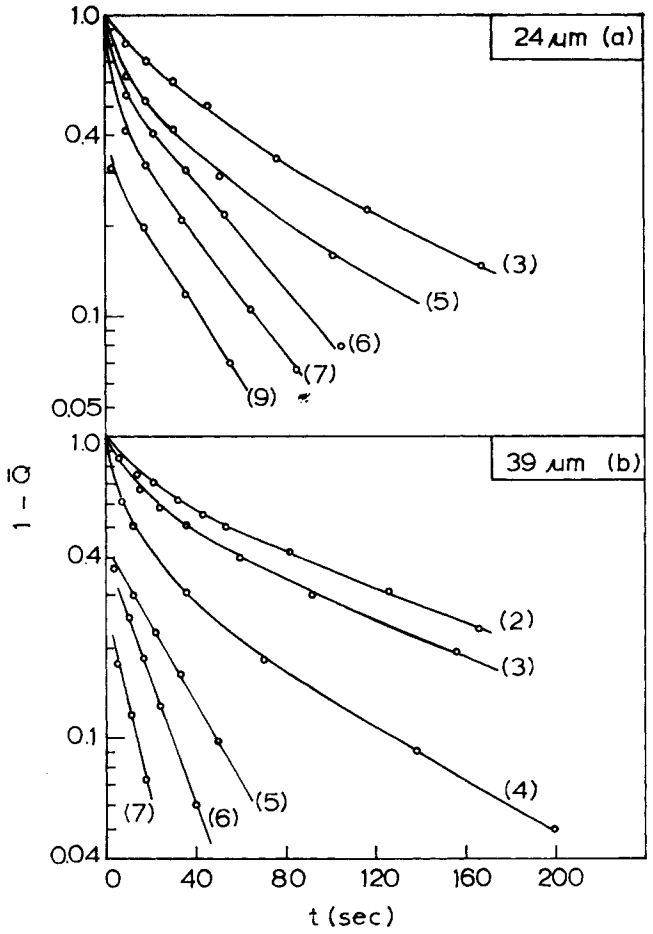

Figure 6. Uptake curves for iso-octane in 13X zeolite crystals at 403°K showing transition from isothermal diffusion at low pressures to heat transfer control at higher pressures. (a) 24μm crystals, (b) 39 μm crystals. Theoretical curves for runs 2b and 3a are from Eq. 9 (isothermal diffusion). Curves for all other runs are from Eqs. 6 and 8 with parameters given in Table 4. Run numbers are given in parenthesis.

$$\beta \equiv \frac{\Delta H}{C_p} \cdot \frac{\partial q^*}{\partial T} = \frac{q}{(C_p/R)} \cdot \left(\frac{\Delta H}{RT}\right)^2 \tag{13}$$

and it is evident that as $q \to o$, $\beta \to o$. At sufficiently low sorbate concentrations the uptake curve will, therefore, be controlled by isothermal diffusion. If the isotherm can be represented by a simple Langmuir expression ($q = Kc(1 + Kc/q_m)^{-1}$) then:

$$\beta = \left(\frac{\Delta H}{RT}\right)^2 \cdot \frac{q_m}{(C_p/R)} \cdot \theta(1 - \theta) \tag{14}$$

and it follows that β also approaches zero in the saturation region ($\theta \to 1$). The intrusion of heat transfer resistance is, therefore, most important in the intermediate concentration region.

The transition observed in Figure 6, from near isothermal diffusion at low pressures to an increasing degree of heat transfer control at higher pressures, is therefore in accordance with theory. It is also evident from Eq. 5 that in the saturation limit the effective diffusivity will become very large, so that in this region the uptake rate may become too fast to measure.

To analyze the uptake curves obtained under conditions such that both diffusion and heat transfer resistances are significant, values of β were calculated from the equilibrium data using the values of C_p derived (for similar sample weights) from the uptake curves measured under conditions of complete heat transfer control with a faster diffusing sorbate ($C_p \approx 1.88$ J/g · deg for 12-14 mg samples and $C_p \approx 1.63$ J/g · deg for 20 mg samples.

The value of p_1 was then found from the intercept of the plot of $\ln(1 - \bar{Q})$, Figure 1, and the value of D_e/l^2 was then calculated from the slope of the $\ln(1 - \bar{Q})$ vs. t plot in the long time region. Values of α and $ha/\rho c_s$ were then calculated according to Eq. 8. For those uptake curves for which the initial uptake rate was slow enough to measure the initial values of D_e/l^2 derived by fitting the uptake curve to the isothermal diffusion model (Eq. 9) agreed well with the values derived from the nonisothermal analysis of the tails of the uptake curves.

In several cases, the parameter values were further refined by optimizing the fit of the uptake curve to Eq. 6, using as initial estimates the values of D_e/l^2 and $ha/\rho C_p$ derived in the above manner. A representative set of parameter values derived from the analysis of one set of uptake curves is given in Table 4. The agreement between the experimental and theoretical uptake

TABLE 4. PARAMETERS DERIVED FROM ANALYSIS OF NONISOTHERMAL UPTAKE CURVES HAVING SIGNIFICANT MACRODIFFUSIONAL RESISTANCE

Run No.	$p_1 - p_2$ (Pa)	q (molecules/cage)	β	α	D_e/l^2 (s^{-1})	D/l^2 (s^{-1})	$ha/\rho C_p$ (s^{-1})
			Iso-Octane at 403°K in 39μm 13X—12-mg Sample				
1	0.27-1.1	0.65	0.36	—	0.0035	7200	Isothermal
2	1.1 -2.7	1.15	0.51	—	0.005	4280	Isothermal
3	2.7 -4.4	1.32	0.46	1.3	0.018	4600	0.02
4	4.4 -8.5	1.45	0.37	1.33	0.038	3100	0.05
5	8.5 -15	1.54	0.29	1.44	0.05	1600	0.07
6	15-24	1.59	0.25	0.74	0.01	2000	0.09
7	24-33	1.63	0.2	0.65	0.15	1600	0.10
			Iso-Octane at 403°K in 24μm 13X—12-mg Sample				
3	0.27-0.6	0.36	0.22	—	0.0044	4200	Isothermal
5	2.1 -2.9	1.07	0.53	1.9	0.014	6000	0.03
6	2.9 -4.0	1.2	0.51	1.8	0.017	5000	0.03
7	4-5.3	1.28	0.49	1.4	0.03	4000	0.04
			Cyclohexane at 409°K in 10X—51-mg Sample				
	187-205	0.366	0.18	0.455	0.051	234	0.023
	536-602	0.872	0.333	0.883	0.026	81	0.023
	946-1053	1.274	0.381	1.174	0.02	38	0.023
	1680-1493	1.65	0.367	0.97	0.027	28	0.026
	2600-2879	1.93	0.32	0.95	0.031	15	0.03
	3532-3900	2.06	0.284	0.77	0.041	12	0.031
	3900-4370	2.1	0.275	0.85	0.035	8.7	0.03

C_p = 1.9 J/g · deg for 12-mg sample and 1.63 cal/g · deg for 51-mg sample. Pan diameter ~ 0.7 cm.

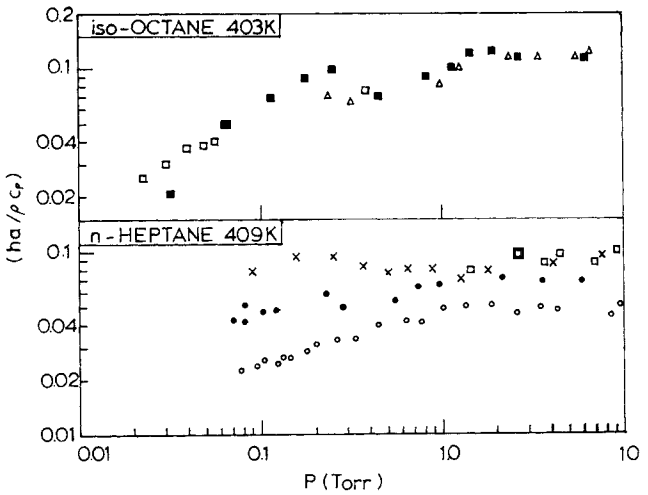

Figure 7. Variation of heat transfer time constant ($ha/\rho C_p$) with sorbate pressure. (× 22 mg Linde 13X; ○ 20 mg 17μm; 28 mg 17μm on wide pan; 14 mg 39μm □; 14 mg 24μm ■; 14 mg 55μm) (1 torr = 133.3 Pa).

curves is excellent, as may be seen from Figure 6, and the values obtained for the heat transfer parameter $ha/\rho C_p$ agree well with the values obtained with similar samples under conditions of complete heat transfer control.

Values of $ha/\rho C_p$ derived from uptake curves measured with similar sample weights and pan diameters are shown in Figure 7 as a function of pressure. The values for both sorbates (*n*-heptane and iso-octane) are consistent. At higher pressures, the values are almost independent of pressure but at lower pressures there is a significant decrease. Both conduction and radiation contribute to the heat transfer. The contribution from radiation is independent of pressure and at higher pressures the thermal conductivity of the gas also becomes independent of pressure so that a constant heat transfer coefficient is to be expected. At pressures less than about 1 torr (Knudsen region) the thermal conductivity of gases decreases rapidly (for example, Dushman, 1962) so that, in agreement with the experimental observation, a significant drop in heat transfer coefficient at low pressures is to be expected. The values of $ha/\rho C_p$ do not vary greatly with temperature but when the values for a given bed were compared over a wide temperature range a small increase was observed, as is to be expected from the temperature dependence of the heat transfer coefficient, Table 6.

Values of D_e/l^2 derived from the uptake curves for iso-octane in 13X (and for cyclohexane in 10X) are shown plotted against sorbate concentration in Figure 8. The behavior is complex, reflecting the fact that the effective diffusivity is a lumped parameter which depends on both the isotherm shape and the molecular and Knudsen diffusivities.

Values of D/l^2 were calculated from the experimental values of D_e/l^2 according to Eq. 5 using the values of $\partial q^*/\partial c$ calculated from the equilibrium isotherms and assuming 50% voidage of the loosely packed sample bed. The values so obtained are plotted against pressure in Figure 9. The temperature dependence of D/l^2 is not strong and is obscured by the experimental scatter but the pressure dependence is striking. Data obtained with different crystal sizes showed no significant difference and, more importantly, the data for four different sorbates (*n*-heptane, iso-octane, benzene and cyclohexane) all lie close to a single curve. At higher pressures (>~67 Pa) D/l^2 decreases inversely with the first power of the pressure while at low pressures D/l^2 appears to approach a constant value.

This behavior is entirely consistent with theoretical expectation since at high pressures the dominant mechanism of transport within the sample bed will be molecular diffusion, with possibly some contribution from forced flow, while at low pressures Knudsen flow will dominate leading to a diffusivity which is independent of pressure. The observed agreement between the experimental diffusivities for different sorbates

TABLE 5. COMPARATIVE UPTAKE CURVES FOR SORPTION IN 10X AND 13X ZEOLITE CRYSTALS UNDER CONDITIONS OF BED DIFFUSION CONTROL (FIGURE 10)

Curve No.	Temp (°K)	Sorbate	Zeolite	Pressure Step (Pa)	2r (μm)	Sample wt. (mg)	Time for 90% Uptake(s)
1	409	C_6H_{12}	10X	600-530	3	42	78
2			13X	500-630	17	20	38
3	438	nC_6H_6	10X	1300-1120	3	63	60
4			13X	1170-1400	17	20	24
5	409	nC_7H_{16}	13X	107-133	17	20	44

Pan diameter ~0.7 cm in all cases.

(having similar molecular diffusivities) and for different sizes of zeolite crystal provides strong evidence that the uptake rate for these systems are indeed controlled by bed diffusion.

SORPTION OF BENZENE AND CYCLOHEXANE IN 10X CRYSTALS

A somewhat less detailed investigation of the kinetics of sorption of benzene and cyclohexane in small commercial 10X zeolite crystals was also undertaken. As with the 13X systems, the uptake rates were found to be independent on sample bed depth indicating the dominance of bed diffusion rather than intracrystalline diffusion resistance. A comparison of uptake curves measured under similar conditions with large 13X and small 10X crystals is shown in Figure 10 and Table 5. Uptake rates in the small 10X crystals are slower than in the large 13X crystals but this difference appears to be due to the difference in adsorbent sample bed depth, rather than to any difference in intracrystalline diffusivity.

The uptake curves were analyzed in the same way and one representative set of data for the 10X system is included in Table

TABLE 6. COMPARISON OF EXPERIMENTAL AND THEORETICAL HEAT TRANSFER COEFFICIENTS FOR SORPTION IN 10X AND 13X ZEOLITE CRYSTALS

	Calculated Values			Experimental Values	
T (°K)	$h'' \times 10^4$ (J · cm^{-2} · s^{-1} · deg^{-1})	$h' \times 10^4$ (J · cm^{-2} · s^{-1} · deg^{-1})	$h \times 10^4$ (J · cm^{-2} · s^{-1} · deg^{-1})	ha (J · cm^{-2} · s^{-1} · deg^{-1})	ha (J · cm^{-2} · s^{-1} · deg^{-1})
		Cyclohexane—10X			
353	6.44	8.0	14.4	0.046	0.042
377	7.56	9.6	17.2	0.054	0.054
409	9.0	12.4	21.2	0.067	0.071
438	10.4	15.5	26.0	0.079	0.084
488	12.8	21.1	34.0	0.10	0.105
		Benzene—10X			
411	7.6	8.6	19.9	0.050	0.05
438	7.7	15.8	23.4	0.06	0.054
478	10.6	19.9	30.5	0.075	0.058
517	12.2	25.3	37.5	0.092	0.075
		Cyclohexane—13X			
409	12.1	12.4	24.5	0.19	0.18
438	14.0	15.8	29.5	0.23	0.22
458	15	17.1	32.2	0.25	0.25
488	17.3	21.1	38.5	0.29	0.29

Contribution from radiation (h') is calculated according to Stefan's Law assuming an emissivity of 0.8; $h' = 18.2 \times 10^{-12} T^3$ (J · cm^{-2} · s^{-1} · °C). Contribution from conduction (h'') is estimated assuming the pan of sieve can be represented by a spherical particle of the same volume as the adsorbent: $h'' = k/R$, where R is the radius of the equivalent sphere. A bed voidage of 0.5 and crystal density of 1.6 g/mL is assumed with an external surface area of 2 cm^2.

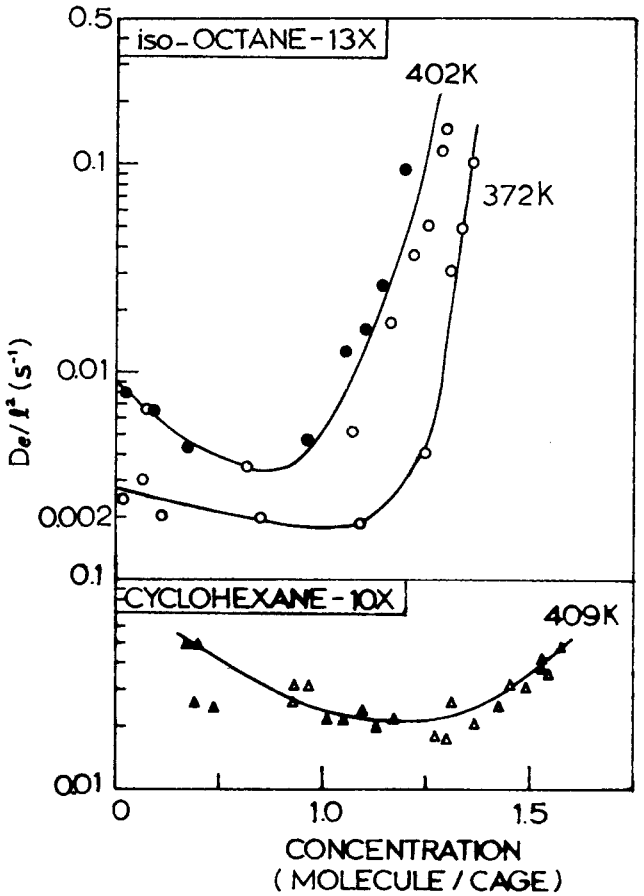

Figure 8. Variation of effective diffusional time constant (D_e/l^2) with sorbate concentration. (●, 24μm; ○, 39μm 13X. ·, 3μm 10X).

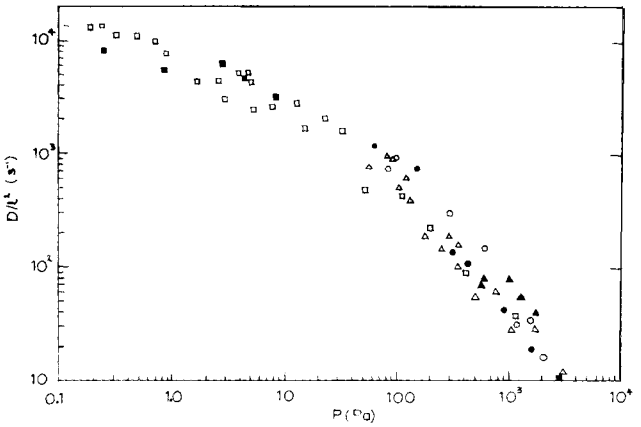

Figure 9. Pressure dependence of macrodiffusional time constant (D/l^2) for sorption in 13X zeolite. Data are for temperatures within the range 370-430°K with comparable sample bed depths. iso-octane (39μm crystals, □; 24μm crystals, ■. *n*-heptane 39μm crystals, ▲; 17μm crystals, ·; benzene (17μm crystals), ●; cyclohexane (17μm crystals), ○) (1 torr = 133.3 Pa).

4. Similar data were obtained for each sorbate at each experimental temperature. While there is considerable scatter, the values of $ha/\rho C_p$ are consistent, show no significant pressure dependence and are in general somewhat smaller than the values obtained at the same temperature for the 13X systems. This difference is consistent with the difference in sample volumes.

The values of ha determined from the experimental values of $ha/\rho C_p$ are compared in Table 6 with values estimated theoretically as the sum of the contribution due to radiation and conduction in a stagnant fluid. Although the method of calculation is

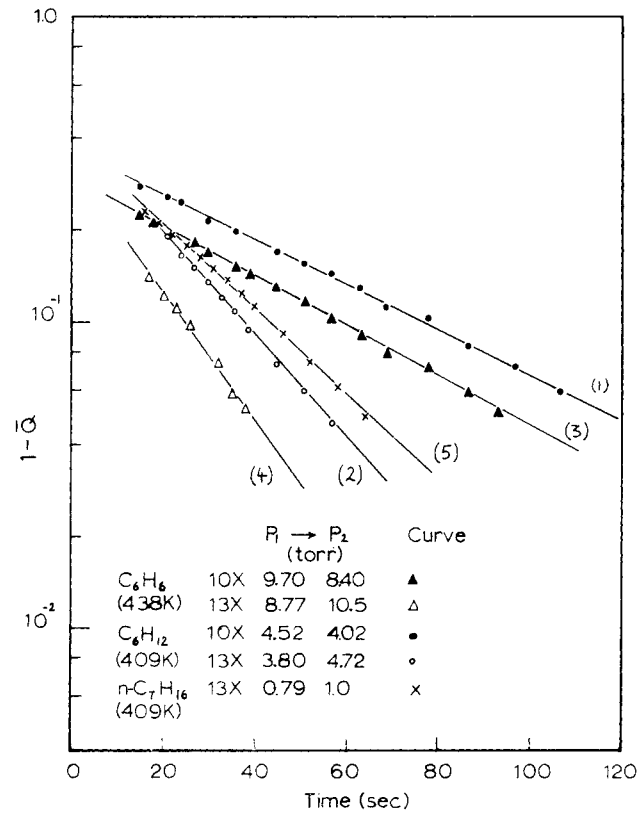

Figure 10. Comparison of experimental uptake curves for 10X and 13X zeolites.

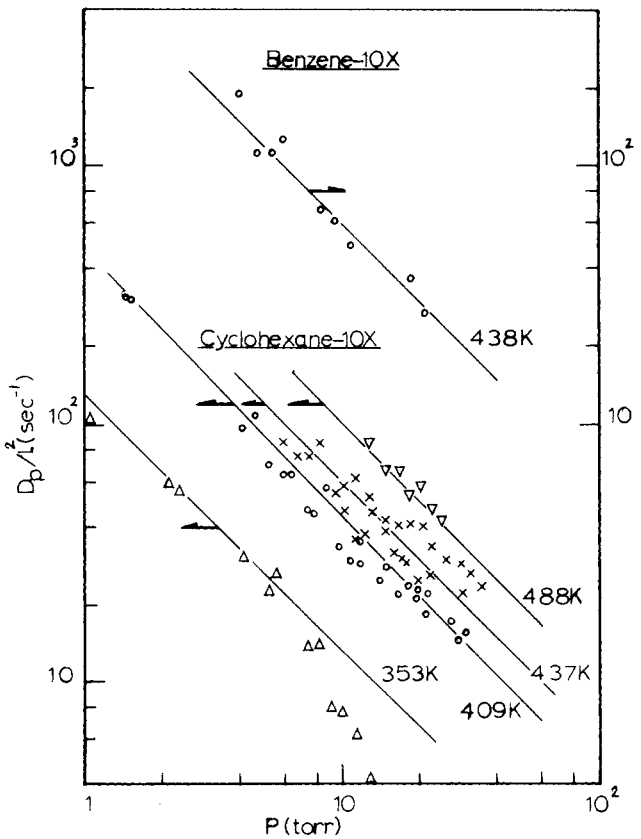

Figure 11. Log-log plot showing inverse dependence of diffusional time constant (D/l^2) on pressure, suggesting the dominance of molecular diffusion as the transport mechanism within the sorbent bed (1 torr = 133.3 Pa).

TABLE 7. COMPARISON OF DIFFUSION COEFFICIENTS FOR DIFFUSION IN A BED OF 10X ZEOLITE CRYSTALS

T (°K)	D/l^2 (s^{-1})	D'_m($cm^2 \cdot s^{-1}$) Experimental Values	Theoretical Values
		Cyclohexane—10X	
353	0.171	0.014	0.037
377	0.302	0.024	0.043
409	0.580	0.046	0.050
437	0.790	0.063	0.057
488	1.32	0.105	0.070
		Benzene—10X	
411	0.45	0.036	0.062
438	0.79	0.063	0.067
478	1.58	0.126	0.081

Values of D/l^2 are corrected to 1 atm. pressure assuming $D \propto 1/P$. Experimental values of D_m are calculated assuming $l = 0.2$ cm and a tortuosity factor of 2, i.e., $D_m = 2 \times 0.2^2 (D/l^2)$.

approximate it is evident that there is good agreement and the observed temperature dependence of the heat transfer coefficient is correctly predicted.

There are in principle three possible transport mechanisms by which the sorbate can penetrate the macropores of the sample: molecular diffusion, Knudsen diffusion and Poiseuille flow. Values of D/l^2 were calculated from the diffusional time constants D_e/l^2 according to Eq. 5 using the values of $\partial q^*/\partial c$ derived from the equilibrium isotherms. The values so obtained are shown plotted against sorbate pressure on logarithmic coordinates in Figure 11. It is evident that D is inversely proportional to pressure suggesting that molecular diffusion is the dominant transport mechanism. The values of D/l^2 are smaller than the values obtained for the 13X systems reflecting the difference in sample size. Furthermore, the data do not extend to pressures below 1 torr so the transition to Knudsen diffusion is not observed.

Values of D'_m (the molecular diffusivity at atmospheric pressure) were estimated from the experimental values of D on the assumption that molecular diffusion is dominant and the values so obtained are compared in Table 7 with the actual values of D'_m calculated from the Chapman-Enskog equation (for example, Hirschfelder, Curtis and Bird, 1954). It is evident that there is order of magnitude agreement although the temperature dependence of the experimental values is somewhat stronger than the temperature dependence of the molecular diffusivity. This may suggest some additional contribution from another transport mechanism such as forced flow, but in view of the numerous approximations it is perhaps surprising that the agreement is as close as it is.

DISCUSSION AND CONCLUSIONS

The results of the experiments with different sizes of adsorbent crystal and different sample configurations show quite clearly that uptake rates in these systems are controlled by heat transfer and macrodiffusion rather than by intracrystalline diffusion. Transport into the adsorbent bed apparently occurs mainly by molecular diffusion, except at very low pressures, and the heat capacities, molecular diffusivities and heat transfer coefficients derived from the uptake curves according to the nonisothermal model are in reasonable agreement with estimated values. In a previous study (Ruthven and Doetsch, 1976), we reported diffusivities for several hydrocarbons in 13X zeolite crystals, derived from the experimental uptake curves assuming an essentially isothermal system with intracrystalline diffusion control.

As a result of the additional experimental evidence reported here, it seems clear that in these earlier experiments the uptake rates were probably controlled by heat transfer and macrodiffusion, rather than by intracrystalline diffusion and the diffusivity values derived cannot therefore be considered reliable. Even smaller diffusivities for light hydrocarbons in type X zeolites have been previously reported by other authors (for example, Ma and Lee, 1976) and it seems likely that in these cases also the uptake rates may have been controlled by processes other than intracrystalline diffusion.

To determine unequivocally the nature of the rate-controlling process in a transient adsorption experiment requires a careful series of preliminary experiments in which the sample configuration and preferably also the adsorbent crystal size are varied. This appears to have been done in very few of the earlier kinetic studies.

A similar conclusion concerning the dominance of macrodiffusion and heat transfer resistance was reported recently by Karger et al. (1978) and by Zikanova et al. (1979) from a study of the sorption kinetics of C_6 hydrocarbons in thin compacts of small 13X zeolite crystals. The measured effective intercrystalline diffusivities were shown to be in satisfactory agreement with the values deduced from NMR measurements. The present study shows that macroresistances are still dominant even in larger crystals of up to 40 μm diameter and the transition from the Knudsen region to the region of molecular diffusion is clearly evident.

The NMR studies also show that intracrystalline diffusion of hydrocarbons in 13X zeolite may be much faster than the values previously reported from sorption kinetic measurements. In a recent study of self-diffusion of alkane hydrocarbons in 13X by the pulsed field gradient method Karger, Pfeifer, Rauscher and Walter (1978), obtained diffusivities in the range 10^{-5}-10^{-6} $cm^2 \cdot s^{-1}$ for heptane and octane at temperatures of 300-400°K. These values correspond to sorption half times in 40-μm crystals of 0.1-0.01 s, which is very much shorter than the time required for macrodiffusion. The results of this study that, even in relatively large (39 μm) crystals of 13X zeolite, intracrystalline diffusion of n-heptane and iso-octane is too fast to measure in an uptake rate experiment, are therefore not inconsistent with the evidence from NMR.

From the practical point of view, the important conclusion is that the sorption rates of medium-sized hydrocarbon molecules in 13X zeolite are unlikely to be significantly affected by intracrystalline diffusion under any normal process conditions. In the analysis of sorption rate data for such systems, intracrystalline diffusion can therefore be safely ignored and it is necessary to consider only intercrystalline diffusion and heat transfer resistances.

ACKNOWLEDGMENT

The experimental uptake curves were obtained in these laboratories by I. H. Doetsch, A. Vavlitis and A. Graham.

NOTATION

a = external surface area per unit volume of adsorbent sample (cm^{-1})
c = gas-phase sorbate concentration (mol/mL)
C_p = effective heat capacity of adsorbent sample and containing pan ($J \cdot g^{-1} \cdot deg^{-1}$)
D_c = intracrystalline diffusivity ($cm^2 \cdot s^{-1}$)
D = diffusivity in macroporous crystal bed ($\approx D_m/\chi$) ($cm^2 \cdot s^{-1}$)
D_e = effective macrodiffusivity in crystal bed [$(\equiv \epsilon D/(1-\epsilon)(\partial q^*/\partial c)$] ($cm^2 \cdot s^{-1}$)
D_c = intracrystalline diffusivity ($cm^2 \cdot s^{-1}$)
D_m = molecular diffusivity ($cm^2 \cdot s^{-1}$)
D'_m = molecular diffusivity corrected to 1 atm. pressure ($cm^2 \cdot s^{-1}$)
h = overall heat transfer coefficient ($J \cdot cm^{-2} \cdot s^{-1} \cdot deg^{-1}$)
K = Henry's Law constant defined by $q^* = Kc$
l = depth of adsorbent sample (cm)

p_n = roots of Eq. 8
P = total pressure in system
q = adsorbed-phase concentration expressed on an intracrystalline basis (mol sorbate/g crystal)
q^* = equilibrium value of q
q_o, q_∞ = initial and final steady values of q
q_m = saturation value of q in Langmuir equation
q_s = value of q at crystal surface
$\bar{q}$ = average value of q through the adsorbent bed
Q = defined in Eq. 6
r = equivalent radius of zeolite crystal (cm)
T = sample temperature (°K)
T_o = initial value of T
t = time (s)
y = distance from surface of adsorbent bed (cm)
$-\Delta H$ = heat of sorption (J/mol)
ρ = density of zeolite crystal (g/mL)
ϵ = voidage of adsorbent sample
τ = dimensionless time variable, $D_e t/l^2$
α = $(ha/\rho C_p)\,(D_e/l^2)^{-1}$
β = $\dfrac{\Delta H}{C_p} \cdot \dfrac{\partial q^*}{\partial T}$
χ = tortuosity factor
θ = fractional coverage ($\equiv q/q_m$)

LITERATURE CITED

Armstrong, A. A., J. D. Wellons, and V. Stannett, "Temperature Effects During Sorption and Desorption of Water Vapour in High Polymers," *Die Makromolekulare Chemie*, **95**, 78 (1966).

Charnell, J. F., "Growth of Large Crystals of NaA and NaX Zeolites," *J. Crystal Growth*, **8**, 29 (1971).

Crank, J., *Mathematics of Diffusion*, Oxford University Press, London, 45 (1956).

Dushman, S., *Scientific Foundation of Vacuum Technique*, John Wiley, New York, 45 (1962).

Hirschfelder, J. O., C. F. Curtiss, and R. B. Bird, "Molecular Theory of Gases and Liquids," John Wiley, New York, 539 (1954).

Karger, J., Pfeifer, H., M. Rauscher, and A. Walter, "Stelbstdiffusionsverbalten der homologen Reihe der n-Alkane van n-Butane bis n-Oktadekan in NaX-Zeolithen," *Z. Phys. Chem.*, Leipzig, **259**, 784 (1978).

Karger, J. et al., "Intercrystalline Molecular Transport in Zeolites Studied by Uptake Experiments and NMR Pulsed Field Gradient Techniques," *J. Chem. Soc. Faraday Trans I*, **74**, 1210 (1978).

Lee, Lap-Keung and D. M. Ruthven, "Analysis of Thermal Effects in Adsorption Rate Measurements," *J. Chem. Soc. Faraday I*, **75**, 2406 (1979).

Ma, Y. H. and T. Y. Lee, "Transient Diffusion in Solids with a Bipore Distribution," *AIChE J.*, **22**, 147 (1976).

Ruthven, D. M. and I. H. Doetsch, "Diffusion of Hydrocarbons in 13X Zeolite," *AIChE J.*, **22**, 882 (1976).

Ruthven, D. M., Lap-Keung Lee, and H. Yucel, "Kinetics of Non-Isothermal Sorption in Molecular Sieve Crystals," *AIChE J.*, 16 (Jan., 1980).

Zikanova, A. et al., "Diffusion of C_6 Hydrocarbons in NaX Zeolites," Symposium on Properties and Application of Zeolites, London (April 18-20, 1979) (Proceedings to be published by Chem. Soc. London).

Manuscript received January 2, 1980; revision received October 8, and accepted October 20, 1980.

Hydrogenolysis and Hydrogenation of Dibenzothiophene Catalyzed by Sulfided $CoO\text{-}MoO_3/\gamma\text{-}Al_2O_3$: The Reaction Kinetics

D. H. BRODERICK

and

B. C. GATES

Center for Catalytic Science and Technology
Department of Chemical Engineering
University of Delaware
Newark, DE 19711

SCOPE

Upgrading of heavy petroleum fractions and synthetic fuels requires high-pressure catalytic hydroprocessing, whereby sulfur-containing organic molecules react with H_2 at (10-20) × 10^6 Pa to produce H_2S and desulfurized organic products. Thiophenic compounds such as the three-ring dibenzothiophene and the four-ring benzo(*b*)naphtho(2,3-*d*)thiophene represent the least reactive sulfur-containing constituents of heavy feedstocks and are, therefore, the key components in determining process kinetics.

The reaction network involving hydrodesulfurization and hydrogenation of dibenzothiophene has been determined under conditions similar to those of commercial processes (573°K and 10^7 Pa) (Houalla et al., 1978). The results presented here include the kinetics of dibenzothiophene hydrodesulfurization and hydrogenation under similar conditions [548-598°K and 1.8 × 10^7 Pa]. Data were obtained for fresh, stable, sulfided $CoO\text{-}MoO_3/\gamma\text{-}Al_2O_3$ (American Cyanamid HDS 16A) with an isothermal piston-flow reactor operating at steady state.

Rates were determined from differential conversion data for hydrodesulfurization and hydrogenation of dibenzothiophene, with the concentrations of the following compounds (in units of kg mol/m^3) having been varied systematically over the ranges indicated: dibenzothiophene (0.008-0.13), H_2 (0.076-0.30), biphenyl (0.00-0.08), and H_2S (0.001-0.068). The results represent the first thorough, quantitative determination of the kinetics of high-pressure catalytic hydroprocessing reactions.

D. H. Broderick is presently with the Chevron Research Co., Richmond, CA 94802. Correspondence concerning this paper should be addressed to B. C. Gates.

0001-1541-81-4800-0663-$2.00.